BROOKHAVEN NATIONAL LABORATORY

BNL-101090-2012-IR

Effect of Sodium Carboxymethyl Celluloses on Water-catalyzed Self-degradation of 200^{0}C-heated Alkali-Activated Cement

T. Sugama, T. Pyatina

May 2012

Sustainable Energy Technologies Department/Energy Conversion Group

Brookhaven National Laboratory

U.S. Department of Energy
DOE office of Energy Efficiency and Renewable Energy

Notice: This manuscript has been authored by employees of Brookhaven Science Associates, LLC under Contract No. DE-AC02-98CH10886 with the U.S. Department of Energy. The publisher by accepting the manuscript for publication acknowledges that the United States Government retains a non-exclusive, paid-up, irrevocable, world-wide license to publish or reproduce the published form of this manuscript, or allow others to do so, for United States Government purposes.

DISCLAIMER

This report was prepared as an account of work sponsored by an agency of the United States Government. Neither the United States Government nor any agency thereof, nor any of their employees, nor any of their contractors, subcontractors, or their employees, makes any warranty, express or implied, or assumes any legal liability or responsibility for the accuracy, completeness, or any third party's use or the results of such use of any information, apparatus, product, or process disclosed, or represents that its use would not infringe privately owned rights. Reference herein to any specific commercial product, process, or service by trade name, trademark, manufacturer, or otherwise, does not necessarily constitute or imply its endorsement, recommendation, or favoring by the United States Government or any agency thereof or its contractors or subcontractors. The views and opinions of authors expressed herein do not necessarily state or reflect those of the United States Government or any agency thereof.

Abstract

We investigated the usefulness of sodium carboxymethyl celluloses (CMC) in promoting self-degradation of 200°C-heated sodium silicate-activated slag/Class C fly ash cementitious material after contact with water. CMC emitted two major volatile compounds, CO_2 and acetic acid, creating a porous structure in cement. CMC also reacted with NaOH from sodium silicate to form three water-insensitive solid reaction products, disodium glycolate salt, sodium glucosidic salt, and sodium bicarbonate. Other water-sensitive solid reaction products, such as sodium polysilicate and sodium carbonate, were derived from hydrolysates of sodium silicate. Dissolution of these products upon contact with water generated heat that promoted cement's self-degradation. Thus, CMC of high molecular weight rendered two important features to the water-catalyzed self-degradation of heated cement: One was the high heat energy generated in exothermic reactions in cement; the other was the introduction of extensive porosity into cement.

1. Introduction

A critical operation in assembling and constructing an enhanced geothermal system (EGS) is to create a hydrothermal reservoir in an impermeable rock stratum at temperatures ≥200°C, located at ~ 3-10 km below the ground surface. In this operation, water is pumped down from injection well to stimulate the hot rock stratum. This hydraulic stimulation initiates the opening of existing fractures [1, 2]. The continued pumping of water acting as stimulation fluid causes the fractures to open after which the rock faces shift due to existing shear stress. When the fracture closes back after this stimulation, the irregularities in the rock prevent them from closing completely, resulting in the formation of a permeable fracture flow network. After forming the reservoir, a production well is installed within the fracture's network. Then, the heat transmission fluid as the working fluid from the injection well is transported to the production well through the hot fractured zones; thereafter, it circulates between the injection- and production-wells.

During construction of such a wellbore, the operators pay considerable attention to the preexisting fractures in the rock, and to the pressure-generated ones made in the underground foundation during drilling. These fractures in terms of lost circulation zones often cause the wastage of a substantial amount of the circulated water-based drilling fluid. To deal with this problem, operators first must seal or plug the lost circulation zones with appropriate materials to avoid losses of the drilling fluid. In such drilling and sealing operations, the well's temperatures vary between 70 and 110°C and the common temperature is around 85^{o}C. Thus, the sealing materials are required to possess the appropriate setting time at this temperature, to avoid the undesirable fast setting of sealer during the down-hole pumping operation. Further, the cured sealer must develop an adequate mechanical strength responsible for providing a satisfying plugging performance without its dislodgement from fractures when drilling operation is resumed. Once this problem is resolved, the drilling operation continues until the wellbore structure is completed. Thereafter, the hydraulic–stimulation process begins. Next, all sealing materials used to plug the fractures present in hydrothermal reservoir's rock stratum must be disintegrated by water under high pressure to reopen the sealed fractures for better heat exchange with the hot formation.

Presently, Ordinary Portland Cement (OPC) is used as a well-casing cementing material; it is also often adapted as the binder in the sealing systems [3, 4]. The major drawback of OPC use in corrosive geothermal wells is its limited resistance to the hot acidic environment created by the combination of concentrated dihydrogen sulfide (H_2S) and carbon dioxide (CO_2). As is well documented [5, 6], the capacity of OPCs to withstand acid is very poor, and they suffer from severe acid erosion. To deal with this problem, acid-resistant cements are required. In response to this need, our previous work was devoted to evaluating the susceptibility of alkali-activated cementitious materials (AACMs) to acid erosion [7, 8]. The AACMs were prepared hydrothermally using two major starting materials: One was industrial by-products with pozzolanic properties, such as granulated blast-furnace slag and fly ashes; the other was sodium silicate with various

molar ratios of Na_2O/SiO_2 as the alkali activators that initiates pozzolanic reactions. Two factors contributed to minimizing acid erosion: One was the self-repairing property of the cement itself; the other was the anti-acid zeolite phase formed by the interactions between the fly ash and the Na ions liberated from the sodium silicate activator. From this work, we concluded that these AACMs have a high potential as acid-resistant geothermal well cements at temperatures up to 200°C.

Several biodegradable biopolymers are currently employed as additives for cements self-degradation; they include starch, cellulose acetate, gelatin, and poly(L-lactic acid) in the form of powder, microsphere, and fiber. All of them promote the partial biological degradation of biocompatible bone cements [9-14]. When these additives in the bone cements come in contact with body fluids, they degrade, creating an interconnected pore network structure in the cement, allowing the bone-tissues to grow into inter-connective channels and facilitating the degradation of cement. Further, of particular interest in biopolymers is their intriguing mechanism of thermal degradation. The cellulose and cellulose-related compounds are degraded thermally in air at around 200°C, yielding volatile CO_2 gas and acetic acid vapor as degradation products [15-17]. This information inspired us to investigate the potential of cellulose compounds as thermal degradable additives that would promote the self-degradation of temporary cementitious sealing materials at temperatures ≥200°C after water penetration through the sealer. Sodium carboxymethyl cellulose (CMC) and cellulose-related compounds are not new materials in the well drilling industries. These compounds are frequently used as additives in water-based drilling fluids to reduce fluid loss and to assure appropriate rheological properties at elevated temperature [18-22].

The ideal sealer must not only plug the fractures at a low temperature of 85°C, but also it must self-degrade at the well temperature of ≥200°C. In hot geothermal wells the sealer plugging the fractures may encounter two different environments: One is hydrothermal at the inlet of fracture; the other is hot dry at its end. Thus, the sealer is required to disintegrate under both conditions. For the former condition, its disintegration takes place in hot water at 200°C. In contrast, for the latter, the degradation would occur after the 200°C-heated sealer come in contact with water.

Based upon this concept, our particular interest lay in determining the efficacy of CMC in promoting the disintegration of cementitious sealer under the latter condition. Thus, our focus in this study was centered on assessing the ability of CMCs of different molecular weights to degrade the 200°C-heated AACMs after contact with water, in particular, the sodium silicate-activated slag/Class C fly ash combined cement system. Additionally, we evaluated the effect of CMCs on the setting time of cement's slurry at 85°C and on the compressive strength of cement cured under hydrothermal environment at 85°C. To obtain this information, the study focused on the following six aspects: 1) Investigating the hydration behavior of cement's slurry after incorporating CMCs; 2) determining the changes in compressive strength caused by adding the CMCs; 3) elucidating details of the CMC's thermal decomposition behavior, and their sensitivity to the alkalis in cement; 4) identifying and quantifying the volatile chemical derivatives emanated during the thermal decomposition of CMCs, and the reaction products yielded by the interactions between

CMC and sodium silicate activator; 5) measuring the *in-situ* heat generated in the cement after contact with water; and, 6) visually observing and evaluating the magnitude of their self-degradation. After integrating all this information, we propose the physicochemical factors contributing to the self-degradation of the cement by CMC.

2. Experimental procedure

2.1. Materials

We employed the four different sodium carboxymethyl celluloses (CMCs) under the production names "Walcocel CRT 30 PA, 100 PA, 2000 PA, and 30000 PA", supplied by Dow Chemical Corp, and evaluated their ability to degrade sealer. Two industrial by-products, possessing pozzolanic properties, were used as the hydraulic pozzolana cement: One was granulated blast-furnace slag under trade name "New Cem"; the other was Class C fly ash. The slag was supplied from Lafarge North America, and the fly ash was obtained from Boral Material Technologies, Inc. Their chemical compositions detected by micro energy-dispersive X-ray spectrometer (μ EDX) were as follows: Slag; 38.5 wt% CaO, 35.2 wt% SiO_2, 12.6 wt% Al_2O_3, 10.6 wt% MgO, 1.1 wt% Fe_2O_3, and 0.4 wt% TiO_2; Class C fly ash; 30.2 wt% CaO, 31.9 wt% SiO_2, 21.7 wt% Al_2O_3, 4.6 wt% MgO, 6.1 wt% Fe_2O_3, 1.7 wt% Na_2O, 0.7 wt% K_2O_3, and 3.1 wt% SO_3. An anhydrous sodium silicate granular powder under the trade name "Metso Beads 2048," supplied by The PQ Corporation, was used as the alkali activator of these pozzolana cements; its chemical composition was 50.5 mol. wt % Na_2O and 46.6 mol. wt % SiO_2. The formula of the dry pozzolana cements employed in this test had slag/Class C fly ash ratio of 20/80 by weight. A 10 % of this alkali activator by total weight of pozzolana cement was added to prepare the dry mix cementitious reactant. Further, 1.2 % CMC by the total weight of pozzolana cement was incorporated into this dry mix. In preparing cement slurry with similar consistency, the water/cement (W/C) ratio depended on the particular CMC; namely, the ratio was 0.33, 0.39, 0.51, and 0.75, respectively, for 30 PA-, 100 PA-, 2000 PA-, and 30000 PA-incorporated cement slurries. These slurries were left at room temperature in air until they solidified. Afterward, all set cements were autoclaved at 85°C for 24 hours under a pressure of 1000 psi to prepare the hydrothermally cured cement. Since the ideal sealer not only plugs the fractures at 85°C, but also self-degrades when the well temperature reaches ≥200°C, some 85°C- autoclaved cements were heated for 24 hours in an oven at 200°C, before exposing them to water.

To evaluate the susceptibility of CMCs to alkaline cement slurry at 85° and 200°C, the cement pore solution was extracted from the slurry of sodium silicate-activated 20/80 slag/Class C fly ash cement by centrifuging it at 6000 rpm for 10 min. The pH of extracted pore solution was 13.7. The test samples were prepared in the following manner: First, 0.5 g CMC was immersed into 3 ml pore solution at room temperature; second, pore solution-wetted CMC was autoclaved for 24 h at 85° and 200°C; and, then the pore solution-treated CMC was dried at 100°C for further testing.

2.2. Measurements

The molecular weight (MW) of the "as-received" 30, 100, 2000, and 30000 PA CMCs was measured by High-Performance size-exclusion Chromatography/Laser Light Scattering (HPC/LLS). First, all the CMCs, except for 30000 PA, were dissolved in running buffer at ~3.5 mg/ml concentration, then filtrated through a 200 nanometer Dura-pore membrane. For 30000 PA, we encountered unexpected phenomena that the dissolved 30000 formed a large aggregate, precluding its filtration so that there was no possibility to measure its MW. The High-Resolution Scanning Electron Microscopy (HR-SEM) was used to explore the different morphological features of CMCs along with different MWs. TAM Air Isothermal Microcalorimetry was employed to obtain the initial- and final-setting times and to determine the extent of hydration heat energy evolved during the hydrolysis-hydration of these cementitious slurries at 85°C. The changes in compressive strength for 85°C-24 h-autoclaved cements as a function of CMC's Mw were obtained using Instron Model 5967. The cylindrical (16 mm diameter by 35 mm length) specimens were used for this assessment. Using the helium pyconometry, we measured the porosity of the same sized 85°C-24 h-autoclaved cements containing CMCs of different MWs after heating them at 200°C for 24 hours. We investigated the thermal decomposition-related properties of non- and pore solution treated-CMCs using Thermo Gravimetric Analysis (TGA) at the heating rate of 20°C/min in a N_2 flow. Pyrolysis-Gas Chromatography/Mass Spectroscopy (Py-GC/MS) was employed to identify the chemical states of the volatile derivatives emitted by the decomposition of CMC, and also to obtain the quantitative data of the identified derivatives. To accomplish this, a 5-10 mg sample was pyrolyzed at 450°C by a CDS 2500 Pyrolysis Autosampler, and then, we identified and assessed the volatile chemical compounds and their quantities using an HP 5890 Series II Gas Chromatograph coupled with an HP 5989 Mass Engine. The chromatographic peaks were identified by referencing them to the NIST MS library and data in the literature, and by comparing their chromatographic retention times to those of the available reference chemical compounds. Some solid compounds remain after CMC decomposition. Thus, we adapted Fourier transform infrared (FT-IR) spectroscopy to identify these decomposition products of CMC and to define their reaction products with sodium silicate at 200°C. In preparing the FT-IR samples, the dry mixtures with100/0, 89/11, 86/14, 80/20, 67/33 CMC/sodium silicate ratios by weight were dissolved in a constant amount of water at room temperature, and then these samples were placed in an over at 200°C for 24 hours; thereafter, the dry samples were ground up for FT-IR analysis. Then, using TAM Air Isothermal Microcalorimetry, we monitored the heat flow generated by their reactions with water. Also, microcalorimiter was used to measure *in-situ* heat evolved in a self-degrading process of CMC-modified cement after contacting water.

3. Results and Discussion

3.1. CMCs

We measured the viscosity of the CMC powders dissolved in water. The viscosities for solutions made by dissolving 1g CMC in 200 g water were 200, 300, 1010, and 6950 cp for the "as received" 30 PA, 100 PA, 2000 PA, and 30000 PA, respectively, suggesting

that the increase in number of PA corresponds to an increasing molecular weight (MW) and rising viscosity, while the pH of all CMCs ranged from 7.45 to 7.87. As expected, the MW of 30 PA, 100 PA, and 2000 PA CMCs were determined as 80500, 133400, and 224000, respectively. Thus, we assumed that the MW of 30000 PA is more than 224000. Fig. 1 shows the SEM image of "as-received" 30 PA and 30000 PA CMC powders. They disclosed two distinctive micro-structures: One was agglomerated particles with sizes between 10- and 200-μm; the other was a noodle-like conformation.

3.2. Changes in setting behavior of cement slurry by CMCs

To assess the effect of CMCs on setting of cement slurry at the isothermal temperature of 85°C, we investigated the following two factors based upon TAM microcalorimetry heat flow-time relation curves: One was the initial- and final-setting times of CMC-incorporated cement slurries; the other was the total heat energy evolved in slurries during their hydrolysis and hydration. Fig. 2 depicts the microcalorimeter curves in elapsed times up to 20 hours after the ampoules containing the 30 PA-, 100 PA-, 2000 PA-, and 30000 PA-incorporated slurries were placed in the calorimeter. For 30 PA, the curve revealed the appearance of pronounced single peak shortly after the sample introduction, corresponding to an initial setting time of 37 min and its final-setting time of 10 h 48 min. In contrast, the 100 PA had doublet peak, with the first peak being likely due to potential ionic hydrolysates dissociated from slag and Class C fly ash as pozzolanic cement-forming reactants by the alkalinity of the sodium silicate, and also it might involve the hydrolysis of some sodium silicate. The second peak can be accounted for by a hydration-related energy evolved in the cementitious structure assembled by the interactions between the liberated ionic reactants. Additionally, the initial and final setting times were slightly longer (by 8 and 23 minutes respectively) in comparison with those of 30 PA. A further delay in setting times was observed for 2000 PA-modified cement. They were 10 min and ~ 4 hours longer for initial and final settings respectively in comparison with the 100 PA-modified cement; furthermore, this curve encompassed a shoulder peak assigned to the hydration-related heat evolution. The setting times were dramatically prolonged to 1h 53 min for the initial setting and 19h and 31 min for the final setting in case of the 30000 PA-containing cement

Table 1 summarized all the initial and final setting times described above, and also the evolution of the total energy, J/g, which was computed from the enclosed area of the curve with the baseline made between initial and final setting times. As a result, it appeared that these setting times depended primarily on the MW; namely, the increase in MW considerably delayed these setting times. Furthermore, the total energy tended to decline as MW increased. In fact, a 99.5, 98.3, and 63.9 J/g for 100, 2000, and 30000 PA was equivalent to 12, 13, and 44 % decrease in comparison with that of 30 PA-modified cement.

Table 1. Initial- and final-setting times, and total evolution energy attributed to hydrolysis and hydration at 85°C for 20/80 slag/Class C fly ash ratio sealer slurries containing various CMCs.

CMC	Initial setting time, hr:min	Final setting time, hr:min	Total evolution energy, J/g
30 PA	0:37	10:48	113.0
100 PA	0:45	11:11	99.5
2000 PA	0:55	15:01	98.3
30000 PA	1:53	19:31	63.9

3.3. Compressive strength

Our attention next shifted to correlating the total energy evolved throughout the hydrolysis-hydration reactions to the mechanical behaviors of 85°C-autoclaved cements. Fig. 3 plots the values of compressive strength for cements with the CMCs of different MWs. The data revealed that compressive strength declined with an increase in CMCs' MW; in fact, the average compressive strength of 18.0 MPa for the cement made with the lowest MW (30 PA) fell by nearly 39% to 10.1 MPa, when the highest MW CMC (30000 PA) was used. Since a higher MW lowered the total evolved energy, it appeared to restrain cement hydration reactions and, as a result, the development of the compressive strength.

3.4. TGA study

As described earlier, one inevitable factor affecting the self-degradation of cement was the emanation of gaseous and vaporous species, in particular CO_2 and acetic acid, brought about by thermal decomposition of CMC in the cement body. Hence, it was very important to obtain the quantitative data on the generation of these volatile chemical compounds as a function of temperature. A high rate of such emanation may improve the self–degrading performance of cement. The other consideration was the exposure of CMC to a high alkaline environment at elevated temperature, in cement slurries with pH 13.7. As reported [23], treating cellulose with sodium silicate changes its thermal decomposition properties. Our approach to obtaining this information was to measure the loss in weight of various CMCs treated with pH 13.7 pore solution extracted from cement slurry and to survey their thermal decomposition behaviors, using TGA in a range of 25°-850°C. Assuming an EGS well temperature of 200°C, this treatment was conducted by exposing the CMCs in the pore solution to 200°C for 24 hours. For comparison purpose, we investigated weight loss and thermal decomposition behavior of non-treated and 85°C-24h-treated CMCs.

Fig. 4 shows the TGA curves for "as received" 30, 100, 2000, and 30000 PA CMCs denoted as non-treated ones. The features of these curves closely resembled each other for all CMCs, representing two major thermal decomposition stages: First, at ~ 276°C; and the second at around 603°C. At the end testing temperature of 850°C, the total loss in weight for all CMCs was ~ 81.4 %. When these CMCs were treated with pore solution at

200°C, their TGA curves revealed three major distinctions from those of non-treated ones (Fig. 5): First, all curves represented one major decomposition pattern, wherein the principal weight loss rapidly progressed at temperatures ranging from 25°C to 250°C; second, beyond that, some minor weigh losses occurred in two different temperature ranges, ~400°- ~520°C and ~670°- ~780°C; and, third, the weight loss at the range of 25°-850°C depended on the particular CMC. The first two distinctions strongly suggested that the CMC was very susceptible to a pore solution with a 13.7 pH at 200°C. Such susceptibility promoted the extent of alkali-initiated thermal decomposition of CMC. In other words, the thermal stability of CMC became poor after exposure to a pore solution at 200°C. For the third distinction, Fig. 6 compares the TGA curves for 30000 PA before and after exposure to a pore solution at 200°C. Our particular interest was the fact that the weight loss of treated CMC at 850°C was only 49.1 %, corresponding to 39.7 % less than that of non-treated one at the same temperature. A possible interpretation for this was that of the total CMC amount, 39.7 % was eliminated as volatile gaseous and vaporous during its treatment at 200°C for 24 hours. For the other CMCs, the volatile product-related weight loss after exposure was 34.2, 37.5, and 44.5 % for 30, 100, and 2000 PA, suggesting that higher MW CMC emitted more volatile derivatives.

Based upon TGA curves, we plotted the weight loss of CMCs, exposed to cement pore solution, at temperatures ranging from 200° to 350°C (Fig. 7). The weight loss increased with the increased MW of CMCs. CMCs with a high MW produced abundant amounts of volatile gaseous and vaporous derivatives. Conceivably, the magnitude of sealer's self-degradation may depend on the amount of such volatile derivatives emanated in cement, with their large release enhancing the magnitude of degradation. Assuming the placement temperature of sealer in wells is at around 85°C, we also studied the thermal decomposition behaviors of CMCs in cement pore solution, exposed to this temperature. The resulting TGA curves (not shown) revealed the features similar to those of non-exposed ones, except for shift in the first decomposition temperature to lower values. For instance, for 30 PA, the first decomposition temperature of non-exposed CMC was shifted from 276°C to 185°C by treating it with pore solution at 85°C. The data also demonstrated that the extent of such shift depended on the MW; an increase in MW minimized this shift. Consequently, the difference between shifted and original temperatures was 91°, 87°, 76°, and 74°C for 30 PA, 100 PA, 2000 PA, and 30000 PA, respectively, underscoring that the sensitivity of a lower MW CMC to pH 13.7 pore solution at 85°C was much higher than that of a high MW. In other words, CMC with a high MW possesses a better thermal stability at this placement temperature.

3.5. Pyrolysis-Gas Chromatography/Mass Spectroscopy (Py-GC/MS) study

As mentioned in the TGA study, the thermal decomposition of all pore solution-treated CMCs was characterized by displaying one major decomposition pattern at temperatures from 25° to 850°C; most of their decomposition was completed at temperatures up to 450°C. Thus, our study next centered on identifying the chemical states of volatile gaseous and vaporous derivatives emanated by CMC's thermal decomposition at 450°C and on obtaining the quantitative data on the major volatile derivatives of these CMCs.

We employed Py-GC/MS to gain this information. Fig. 8 shows the abundance-retention time curve for 30000 PA at a pyrolysis temperature of 450°C. The curve encompassed eleven pyrolysis-induced derivatives; they and their abundance are summarized in Table 2. Among the main derivatives of CMC were 56.2 % CO_2 and acetic acid at 12.3 % in conjunction with the minor derivatives comprising 31.5 %. The similar results with two major decomposition derivatives, CO_2 and acetic acid, from pyrolyzed CMC, was reported by the other investigators [24, 25]. Fig. 9 shows the changes in abundance of both CO_2 and acetic acid derivatives at 450°C as a function of MW. As is evident, the abundance of these derivatives tended to rise with an increasing MW, implying that CMCs with a high MW emitted more of these derivatives. In fact, the abundances of CO_2 and acetic acid for 30 PA with the lowest MW of 80500 were 2.19×10^6 and 0.39×10^6, and these abundances rose by 46.6 % and 79.5 % to 3.21×10^6 and 0.7×10^6, when the MW was increased to >224000 (30000 PA). Thus, this finding strongly supported the earlier TGA data. We believe that CMCs with a high MW would generate plenty of these reactive volatile derivatives in sealer with a high pH, enhancing the cement's self-degradation.

Table 2. Pyrolysis derivatives along with their abundance obtained from Py-GC/MS at 450°C for 300000 PA CMC.

ID Number	Retention time (min)	Compounds	Abundance x 10^6
1	1.95	Carbon dioxide	3.21
2	2.61	Acetic acid	0.70
3	3.36	1-hydroxy-2-propanone	0.32
4	5.92	(2-oxo-3-cyclopenten-1-yl)acetaldehyde	0.20
5	6.99	2-methyl-2-cyclopenten-1-one	0.12
6	8.66	2-hydroxy-3-mehyl-2-cyclopenten-1-one	0.19
7	8.71	3,4,4,-trimethyl-5-oxo-2-hexenoic acid	0.20
8	8.97	2,4-dimethyl-1,3-cyclopentanedione	0.28
9	9.19	3-methyl-phenol	0.14
10	9.45	2-methyl-phenol	0.11
11	9.94	3-trans-diethoxy-5-methylcyclohexane	0.24

3.6. Porosity of cement

Next we measured the porosity of cement created by such volatile derivatives. Figure 10 shows the porosity of 85°C-autoclaved cements containing 30, 100, 2000, and 30000 PA and a control without CMC after heating at 200°C for 24 hours. The porosity of the control cement without CMC was 23.1 %. When the CMC with the lowest MW (30PA) was added to the control, its porosity increased by 19 % to 27.4 %. A further increase in MW caused with increase in porosity; the CMC 30000 PA with the highest MW created 50.5 % porosity, which was more than double that of the control. The development of a highly porous structure can be one of the factors promoting the self-degradation of cement.

3.7. Chemical affinity of CMC with sodium silicate

Although some CMCs in cement convert to volatile species at 200°C, the non-volatile CMC remnants might react with hydrolysates derived from the dissolution of sodium silicate in water. To obtain information on these reactions, we prepared three samples, 100/0, 20/80, and 0/100 CMC (30000 PA)/sodium silicate ratios by weight. In preparing the samples, first, the dry components were dissolved in water, and then these solutions were heated at 200°C for 24 hours to convert them into the solid samples.

Fig. 11 illustrates FT-IR spectra in the wavenumber region, 4000-650 cm^{-1}, of "as-received" and 200°C-heated CMC. Based upon the chemical structure of CMC in conjunction with literature survey [26-29], the spectrum (a) of the "as-received" CMC included several prominent absorption bands at 3270 cm^{-1} attributed to OH stretching vibration, at 2922 cm^{-1} associated with aliphatic C-H stretching vibrations, at 1583 and 1407 cm^{-1} due to C-O asymmetric and symmetric stretching in the carboxylate ion group, $-COO^-$, at 1318 cm^{-1} related to C-OH bending, at 1065 cm^{-1} shoulder referred to ether-related C-O-C stretching in glucosidic unites, at 1019 cm^{-1} assignable to ether-related C-O-C stretching in β-(1,4)-glucosidic and $-CH_2-O-CH_2-$linkage; and 694 cm^{-1} related to Na^+---O^- link stretching in sodium alkoxide group. By comparison, the feature of FT-IR spectrum (b) of the 200°C-heated CMC represented two major differences: One was the changes in the intensity of two ether group-related bands; the other was the appearance of new band at 1690 cm^{-1}, assigned to C=O stretching in carboxylic acid group, -COOH . For the former difference, the shoulder band at 1065 cm^{-1} became the principal band, whereas the intensity of the band at 1019 cm^{-1} strikingly decayed, suggesting that the C-O-C bonds in β-(1,4)-glucosidic and CH_2-O-CH_2-linkage were ruptured at 200°C, while the other ether group in glucosidic unites remained intact. From this information, it is possible to assume that the hydrothermal decomposition of CMC at 200°C forms two derivatives, sodium glycolate and glucosidic acid as shown below.

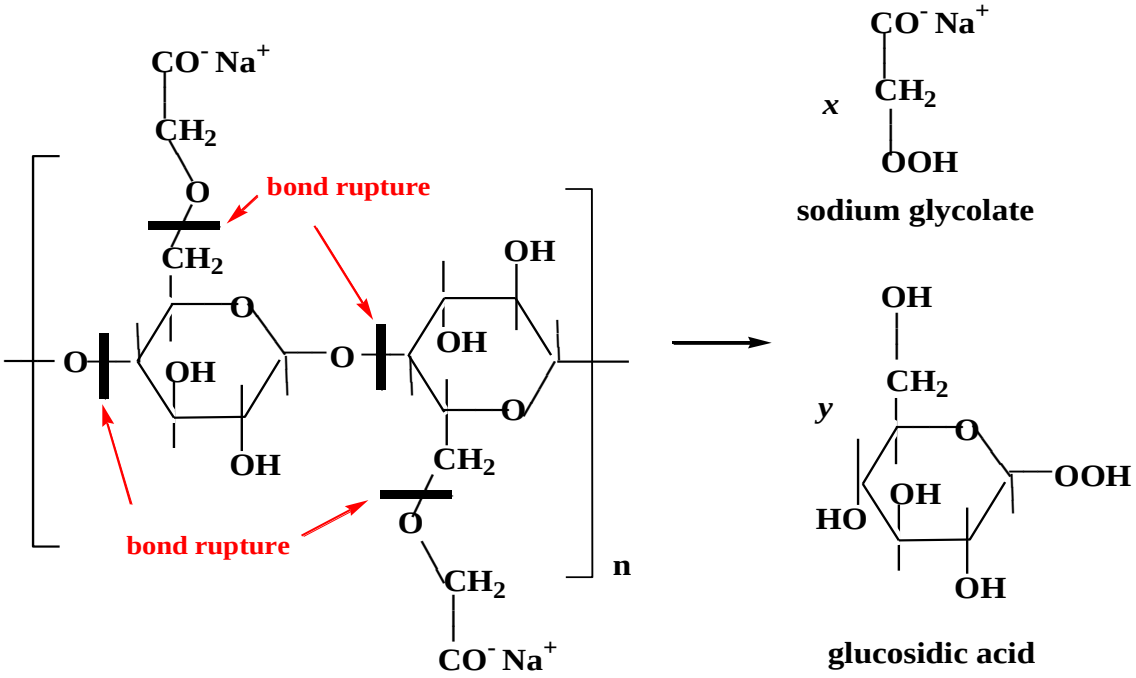

Our focus next shifted to the identification of the CMC and sodium silicate reaction products by FT-IR analysis. Fig. 12 compares the spectral features from 0/100, 100/0, and 20/80 CMC/sodium silicate ratio samples. The spectrum (a) of 200°C-heated bulk sodium silicate encompassed two silicate-related bands at 1025 and 961 cm^{-1}, corresponding to the oxygen-bridging Si-O-Si asymmetric stretching and non oxygen-bridging Si-O^- Na^+ stretching [30, 31], and also two carbonate-related bands at 1445 and 708 cm^{-1}, due to CO_3^{2-} possibly in the sodium carbonate [32, 33]. Thus, since the dissolution of sodium metasilicate in water introduces two hydrolysates, metasilicic acid, H_2SiO_3 and sodium hydroxide, NaOH, the interactions between these hydrolysates during 200°C -heating treatment in the present of an atmospheric CO_2 led to the formation of the sodium polysilicate structure by polycondensation reaction, while the sodium carbonate was derived from the carbonation of NaOH. The proposed hydrolysis, polycondensation, and carbonation reactions of sodium silicate are shown below.

Hydrolysis

$$Na_2SiO_3 + 2H_2O \longrightarrow 2NaOH + H_2SiO_3$$

$$n\text{NaOH} + n\text{H}_2\text{SiO}_3 \xrightarrow{CO_2 \text{ at } 200°C} \text{Na}^+\text{O}^- \quad \text{O}^-\text{Na}^+ \text{ -(-Si-O-Si-)}_n\text{- } \text{Na}^+\text{O}^- \quad \text{O}^-\text{Na}^+ + n\text{Na}_2\text{CO}_3 + n\text{H}_2\text{O}\uparrow$$

When the spectral feature (c) of 20/80 ratio sample was compared with those of 0/100 and 100/0 ratios, there were three major differences: First, the carboxylic acid-related band at 1690 $cm^{-1}$was eliminated; second, the bands at 1407 and 1318 cm^{-1} belonging to the C-O symmetric stretching in the carboxylate ion and the C-OH bending were shifted

to 1427 and 1336 cm^{-1}, respectively; and, third was the appearance of new bands at 1638 and 777 cm^{-1}. The first difference seemingly suggested that the -COOH groups present in sodium glycolate and glucosidic acid derived from the thermal decomposition of CMC were transformed to $–COO^- Na^+$ by their reactions with NaOH hydrolysate from sodium silicate [34, 35]. On the other hand, a possible interpretation of these new bands was the formation of sodium bicarbonate, $NaHCO_3$, [36, 37]. If this latter interpretation is valid, the shifted bands not only were due to these original assignments, but also included the sodium bicarbonates in overlapped bands. Accordingly, we assumed that the interactions between CMC and sodium silicate at 200°C may lead to the formation of the following three water-sensitive reaction products, disodium glycolate salt, sodium glucosidic salt, and sodium bicarbonate as illustrated below, coexisting with some sodium polysilicate and sodium carbonate derivatives as the other water-sensitive compounds from sodium silicate.

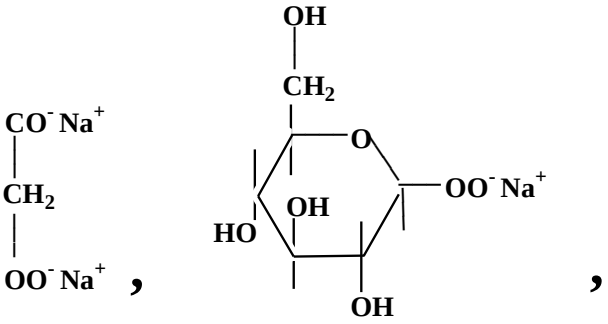

, , and $NaHCO_3$.

Assuming these water-sensitive reaction products being formed in cement at 200°C come in contact with water, we determined the heat energy that would be generated by their hydrolysis. In this test, we employed two controls, bulk CMC and sodium silicate. We mixed 15.4 g of 200°C-heated 100/0, 89/11, 86/14, 80/20, 67/33, 0/100 CMC/sodium silicate ratio samples with 74 g water. After mixing, the maximum heat flow (MHF, W/g) generated by the interactions between samples and water was measured using microcalorimetry (Fig. 13). For the control samples, 0/100 and 100/0 CMC/sodium silicate ratios, the bulk sodium silicate without CMC evolved 1.12 W/g MHF, which was 37.5 % higher than that of bulk CMC, suggesting that two derivatives, sodium polysilicate and sodium carbonate emanate more heat energy after contact with water than two CMC derivatives, sodium glycolate and glucosidic acid. When 11wt% of the sodium silicate was replaced with CMC, denoted as 11/89 ratio, the value of MHF rose by 14.5 % to 1.31 W/g compared with that of 0/100 ratio of CMC/sodium silicate. This finding strongly demonstrated that the water-sensitive reaction products, such as disodium glycolate salt, sodium glucosidic salt, and sodium bicarbonate, were responsible for enhancing exothermic energy. However, further replacement of sodium silicate by CMC like 14/86 ratio engendered some reduction of MHF value. Correspondingly, incorporating more CMC into sodium silicate tended to decline this value. The MHF value for 33/67 ratio was 4.4 % lower than that of 0/100 ratio. Thus, we believe that there is an appropriate CMC to sodium silicate ratio that yields the ideal amount of these reaction products. In this test series, we found that a 11/89 ratio, which was adapted in our study, was the most effective proportion in generating the highest MHF.

To ensure that these water-sensitive reaction products also were formed in the cement, we prepared a 20/80 slag/Class C fly ash ratio cement containing 10 % sodium silicate and 1.2 % CMC (30000 PA) by the total weight of cement as described in the Experimental procedure. The 200°C-heated sample then was analyzed using FT-IR. The FT-IR spectrum (not shown) closely resembled that of the sodium silicate/CMC blended sample without cement, except for the domination of slag- and Class C fly ash-related absorption bands in the wavenumbers, ranging from 1300 to 650 cm^{-1}.

3.8. Self-degradation

Now, we focused on validating the efficacy of these water-sensitive reactants in promoting the self-degradation of 200°C-heated cement after contact with water. Two different tests were conducted to visualize and rationalize self-degradation: First test was the determination of the maximum *in-situ* heat energy evolved in the cement after contact with water; second one was to visually observe the self-degradation of cement after impregnating it with water. In these tests, the 30, 100, 2000, and 30000 PA CMCs were incorporated into sodium silicate-activated cements. We also tested the sodium silicate-activated cement without CMC as control. The detailed test procedures were as follows. For the first test, 1) a certain amount of cement slurry was placed in the glass ampoule, and then autoclaved for 24 hours at 85°C and 6.9 MPa pressure, 2) the cured cement was heated at 200°C for 24 hours, then cooled for 24 hours at room temperature, 3) the cooled cements was weighted, and the samples' weights ranged from 9.06 to 9.25g 3) 8 g water at 22°C were poured on the surface of cooled cement, and 4) immediately after water addition, the ampoule was sealed, and placed in TAM Air Isothermal Microcalorimetry at 22°C to trace the rate of evolved heat flow as a function of elapsed time. For the second test, 1) the cement was autoclaved at 85°C for 24 hours under a pressure of 6.9 MPa, 2) the autoclaved cement was heated at 200°C for 24 hours, 3) the hot cement then was left at room temperature for 24 hours, 4) after cooling, the cement was placed in a vacuum chamber to remove any air present in cement, and 4) the air-free cement was impregnated with water, followed by visual observation of the cement's self-degradation.

Fig. 14 depicts the microcalorimeter curves in the elapsed times up to 100 min for the control, 30-, 100-, 2000-, and 30000 PA CMC-incorporated cements. For all cement samples, the heat flow curve reached the peak within 10 min of the sample introduction into the microcalorimeter. The control sample without CMC had the maximum heat flow (MHF) of 38.8 mW/g, which was related to the dissolution of water-sensitive sodium polysilicate and sodium carbonate compounds derived from the sodium silicate. All the CMCs, except for 30 PA, enhanced the MHF of the cement. The enhancement depended on the MW of CMC; namely, the higher MW resulted in higher *in-situ* heat energy. In fact, the sample with the highest MW CMC, 30000 PA, attained the largest MHF of 102.6 mW/g, corresponding to 2.6-fold increase in comparison with the control. Since the amount of water-sensitive interaction products between CMC and sodium silicate rose with an increasing MW, this was likely the main reason why the CMC with high MW generated such an enhanced *in-situ* exothermic energy. The value of MHF was directly correlated with the magnitudes of the self-degradation performance of the cement. Visual observation from the second test revealed that both the 30000 and 2000 PA cements

contained multiple cracks, compared with 30 PA and the control cements that were only slightly damaged. To further visualize this performance, we tried to gently break these cracked sealers by hand (Fig.14). As is evident from these images, the 30000 and 2000 PA cements crumbled very easily after applying gentle hand pressure to them. Furthermore, the 30000 PA CMC-containing cement broke into much smaller fragments after its self-degradation than that containing CMC 2000 PA.

The experimental results demonstrated that the two factors that played a pivotal role in the self-degradation performance of alkali-activated slag/Class C fly ash blend cement were the development of porous structure with a porosity of 50.5 % by the emission of a large volume of volatile gaseous and vaporous compounds and the high exothermic energy arising from the dissolution of abundant water-sensitive reaction products.

4. Conclusion

The studies were aimed at evaluating the usefulness of sodium carboxymethyl cellulose (CMC) as thermally degradable additive in promoting the self-degradation of 200°C-heated sodium metasilicate-activated slag/Class F fly ash cement system after contact with water and at obtaining the understanding of physicochemical factors contributing to cement's degradation. We explored CMCs of four different molecular weights, 30 PA (80,500 MW), 100 PA (133,400 MW), 2000 PA (224,000 MW), and 30000 PA (>224,000 MW). When CMC was incorporated into cement slurry at 22°C, the slurry's setting time depended on the molecular weight (MW) of CMCs; namely, an increase in MW considerably delayed its setting time from 37 min for 80,500 MW to 113 min for >224,000 MW. Thus, CMC with a high MW delayed the rate of hydrolysis-hydration reactions of cement. Such a decreased reaction rate directly affected the total evolved energy associated with hydrolysis and hydration reactions of cement; the total energy of 63.9 J/g generated from the highest MW was 44 % lower than that of the lowest MW. Correspondingly, the cement made with the highest hydrolysis-hydration energy of 113 J/g developed the highest compressive strength of 21.5 MPa, whereas the cement made with the lowest energy of 63.9 J/g had the compressive strength of only 7.7 MPa.

CMCs were very susceptible to the reactions with alkaline pore solution (pH 13.7) in cement at 200°C. When all CMCs were treated with pore solution at 200°C, the major weight losses measured with TGA ranged from 35 to 44 % and occurred at temperatures below 250°C, compared with only around 10 % weight loss for non-treated ones at these temperatures. Additionally, there was no significant difference for different CMCs in weight loss between 250° and 700°C. The rate of weight loss depended on the MWs; its rate tended to rise with an increase in MW. The major volatile species related to this weight loss were CO_2 gas in conjunction with acetic acid vapor as minor volatile compound. The quantities of CO_2 and acetic acid emitted from CMC with the highest MW at 450°C were 46.6 and 64.1 % higher, respectively, than those from the lowest MW. Correspondingly, the porosity of cured cement significantly increased with an increasing MW, from 27.4 % for 30 AP CMC to 50.5 % for 30000 AP CMC, reflecting the development of a large porosity within the cement's structure. On the other hand, the CMC reacted with NaOH, a hydrolysate of sodium silicate, in an atmospheric

environment containing CO_2 at 200°C, leading to the formation of three water-insensitive solid reaction products, disodium glycolate salt, sodium glucosidic salt, and sodium bicarbonate. The other water-sensitive solid reaction products, such as sodium polysilicate and sodium carbonate, were derived from hydrolysates of sodium silicate at 200°C, while the thermal decomposition of CMC introduced two water-sensitive compounds, glycolate and glucosidic acid. We compared the values of maximum heat flow (MHF) evolved by the dissolution of these water-sensitive derivatives in water at 22°C. This value for the derivatives from sodium silicate was 1.12 W/g, which was 37.5 % higher than from CMC's (30000 PA) derivatives, suggesting that the sodium polysilicate and sodium carbonate evolved more energy during their dissolution than did CMC's derivatives. A further augmentation of dissolution energy was observed from the reaction products between sodium silicate and CMC; in fact, the sample made from 11/89 CMC /sodium silicate ratio generated the MHF of 1.31 W/g, corresponding to 17 % enhancement of energy over the bulk sodium silicate.

When the cements containing these water-sensitive products came in contact with water, the value of MHF evolved by their dissolution depended on MW of CMC; the value rose with an increasing MW. The MHF of 102.6 mW/g from the highest MW (30000 PA) was tantamount to 1.8-, 2.2-, 3.5-, and 2.7-fold increase, compared with that of 2000 PA, 100 PA, 30 PA, and control without CMC respectively. Such high energy was responsible for improving the self-degradation performance of cement. In fact, incorporating 30000 PA most effectively disintegrated the cement into smaller fragments after its self-degradation than did any other CMCs. Thus, the combination of two factors, 1) the exothermic energy occasioned by the dissolution of water-sensitive reaction products and 2) the development of porous structure by emission of abundant volatile compounds, in 200°C-heated cement, played a pivotal role in converting the bulk cement structure into fragments.

References

[1] Kohl T, Megel T. Predictive modeling of reservoir response to hydraulic stimulations the European EGS site Soultz-sous-Forets. In J Rock Mecha Minn Sci 2007; 44: 1118-1131.
[2] Portier S, Vuataz F, Nami P, Sanjuan B, Gerard A. Chemical stimulation techniques for geothermal wells: experiments on the three-well EGS system at Soultz-sous-Forets, France. Geothermic 2009; 38: 349-359.
[3] Fabbri F, Vidali M. Drilling mud in geothermal wells," Geothermic1970; 2: 735-741.
[4] Sugama T, Kukacka LE, Galen B, Milstone NB. Characteristics of high temperature cementitious lost-circulation control materials for geothermal wells. J Mater Sci 1987; 22: 63-75.
[5] Van JHP, Visser S. Influence of alkali on the sulphate resistance of ordinary Portland cement mortars. Cem Conc Res 1985; 15: 485-494.
[6] Irassar EF, Bonavetti VL, Gonzalez M. Microstructural study of sulfate attack on ordinary and limestone Portland cements at ambient temperature. Cem Conc Res 2003; 33: 31-41.
[7] Sugama T, Brothers L. Sodium-silicate-activated slag for acid-resistant geothermal well cements. J.Adv in Cem Res 2004; 16: 77-87.
[8] Sugama T, Brothers L, Van de Putte T. Acid-resistant cements for geothermal wells: Sodium silicate activated slag/fly ash blends. J Adv in Cem Res 2005; 17: 65-75.
[9] Espigares I, Elvira C, Mano JF, Vazquez B, San Roman J, Reis RL. New partially degradable and bioactive acrylic bone cements based on starch blends and ceramic fillers. Biomaterials 2002; 23; 1883-1895.
[10] Boesel LF, Cachinho SCP, Fernands MHV, Reis RL. The in vitro bioactivity of two novel hydrophilic, partially degradable bone cements. Acta Biomaterialia 2007; 3: 175-182.
[11] Zuo Y, Yang F, Wolka JGC, Li Y, Jansen JA. Incorporation of biodegradable electrospun fibers into calcium phosphate cement for bone regeneration. Acta Biomaterialia 2010; 6: 1238-1247.
[12] Habraken WJEM, Liao HB, Zhang Z, Wolke JGC, Grijpma DW, Mikos AG, Feijen J, Jansen JA. In vivo degradation of calcium phosphate cement incorporated into biodegradable microspheres. Acta Biomaterialia 2010; 6: 2200-2211.
[13] Felix Lanao RP, Leeuwenburgh JGC, Wolke JGC, Jansen JA. In vitro degradation rate of apatitic calcium phosphate cement with incorporated PLGA microspheres. Acta Biomaterialia 2011; 7: 3459-3468.
[14] Lopes PP, Garcia MP, Fernandes MH, Fernandes MHV. Acrylic formulations containing bioactive and biodegradable fillers to be used as bone cements: Properties and biocompatibility assessment. Mater Sci Eng 2013; C33: 1289-1299.
[15] Aseyeva RM, Kolosova TN, Lomakin SM, Libonas YY, Zaikov GY, Korshak VV. Thermal degradation of cellulose diacetate, Polym Sci U.S.S.R 1985; 27:1917-1926.
[16] Jandura P, Riedl B, Kokta B.V. Thermal degradation behavior of cellulose fibers partially esterified with some long chain organic acids, Polym. Degrad. Stab., 70 (2000) 387-394.
[17] da Conceicao C. Lucena M, de Alencar AEV, Mazzeto SE, de A. Soares S. The effect of additives on the thermal degradation of cellulose acetate. Polym Degrad Stab 2003; 80: 149-155.

[18] Farbbri F, Vidali M. Drilling mud in geothermal wells. Geothermic 1970; 2: 735-741.
[19] Alldredge AL, Elias M, Gotschalk CC. Effects of drilling mud and mud additives on the primary production of natural assemblages of marine phytoplankton. Marine Envi Res 1986; 19: 157-176.
[20] Dairanieh IS, Lahalih SM. Novel polymeric drilling and viscosifiers. Eur Polym J 1988; 24: 831-835.
[21] Amanullah M, Yu L. Environment friendly fluid loss additives to protect the marine environment from the detrimental effect of mud additives. J Petro Sci. Eng 2005; 48: 199-208.
[22] Dolz M, Jimenez J, Hernandez MJ, Delegido J, Casanovas A. Flow and thixotropy of non-contaminating oil drilling fluids formulated with bentonite and sodium carboxymethyl cellulose. J Petro Sci Eng 2007; 57: 294-302.
[23] Tanzos I, Pokal G, Borsa J, Toth T, Schmidt H. The effect of tetramethylammonium hydroxide in comparison with the effect of sodium hydroxide on the slow pyrolysis of cellulose. J Anal Appl Pyrolysis 2003; 68-69: 173- 185.
[24] Jakab E, Meszaros E, Borsa J. Effect of slight chemical modification on the pyrolysis behavior of cellulose fibers. J Anal Appl Pyrolysis 2010; 87: 117-123.
[25] Torri C, Adamiano A, Fabbri D, Lindfors C, Monti A, Oasmaa A. Comparative analysis of pyrolysate from hebaceous and woody energy crops by Py-GC with atomic emission and mass spectrometric detection. J Anal Appl Pyrolysis (2010); 88: 175-180.
[26] Ibrahim AA, Adel AM, Abd EI-Wahab ZH, Al-Shemy MT. Utilization of carboxymethyl cellulose based on bean hulls as chelating agent. Synthesis, characterization and biological activity. Carbohydrate Poly (2011); 83: 94-115.
[27] Bao Y, Ma J, Li Na. Synthesis and swelling behaviors of sodium carboxymethl cellulose-g-poly(AA-co-AM-co-AMPS)/MMT superabsorbent hydrogel. Carbohydrate Poly (2011); 84: 76-82.
[28] Mishar S, Rani GU, Sen G. Microwave initiated synthesis and application of polyacrylic acid grafted carboxymethyl cellulose. Carbohydrate Poly (2012); 87: 2255-2262.
[29] Peng H, Ma G, Ying W, Wand A, Huang H, Lei Z. In situ synthesis of polyaniline/sodium carboxymethyl cellulose nanorods for high-performance redox supercapacitors. J Powder Sources (2012); 211: 40-45.
[30] Farmer VC and Russell JD. The infra-red of layer silicates. Spectrochimica Acta (1964); 20: 1149-1173.
[31] Uchino T, Sakka T, Iwasaki M. Interpretation of hydrated states of sodium silicate glasses by infrared and raman analysis. J Am Ceram Soc (1991); 74: 306-313.
[32] Soog Y, Goodman AL, McCarthy-Jones JR, Baltrus JP. Experimental and simulation studies on mineral tapping of CO_2 with brine. Energy Conversion and Management (2004); 45:1845-1859.
[33] Trezza MA, Lavat AE. Analysis of the system $3CaO.Al_2O_3$-$CaSO_4.2H_2O$-$CaCO_3$-H_2O by FT-IR spectroscopy. Cem Conc Res (2001); 31: 869-872.
[34] Specht CH, Frimmel FH. An in situ ATR-FTIR study on the adsorption of dicarboxylic acids onto kaolinite in aqueous suspensions. Physical Chemistry Chemical Physics (2001); 3: 5444-5449.

[35] Rosenqvist J, Axe K, Sjoberg S, Persson P. Adsorption of dicarboxylates on nano-sized gibbsite particles: effects of ligand structure on bonding mechanisms. Colloids Surf A: Physicochemical Engineering Aspects (2003); 220: 91-104.
[36] Chen X, Griesser UJ, Te RL, Pfeiffer RR, Morris KR, Stowell JG, Byrn SR. Analysis of the acid-base reactions between solid indomethacin and sodium bicarbonate using infrared spectroscopy, X-ray powder diffraction, and solid-state nuclear magnetic resonance spectroscopy. J Pharmaceutical Bio. Analysis (2005); 38: 670-677.
[37] Nyquist RA, Kagel RO. Infrared spectra of inorganic compounds. New York: Academic press, 1973.

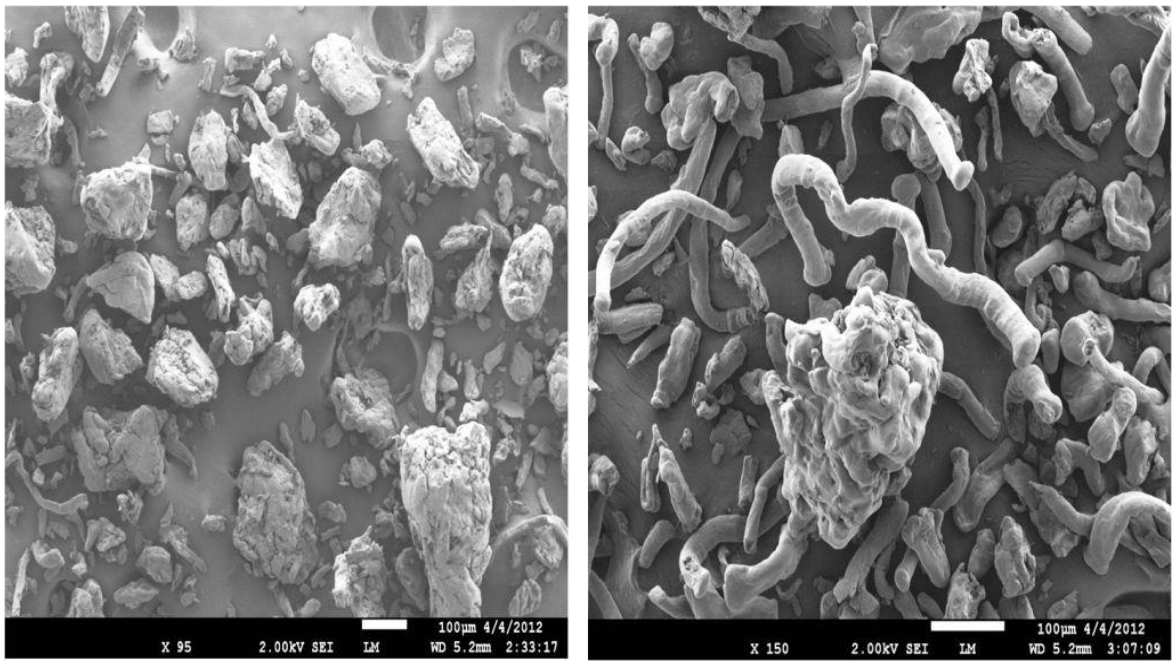

Fig. 1. SEM images of 30 PA (left) and 30000 PA (right) CMCs.

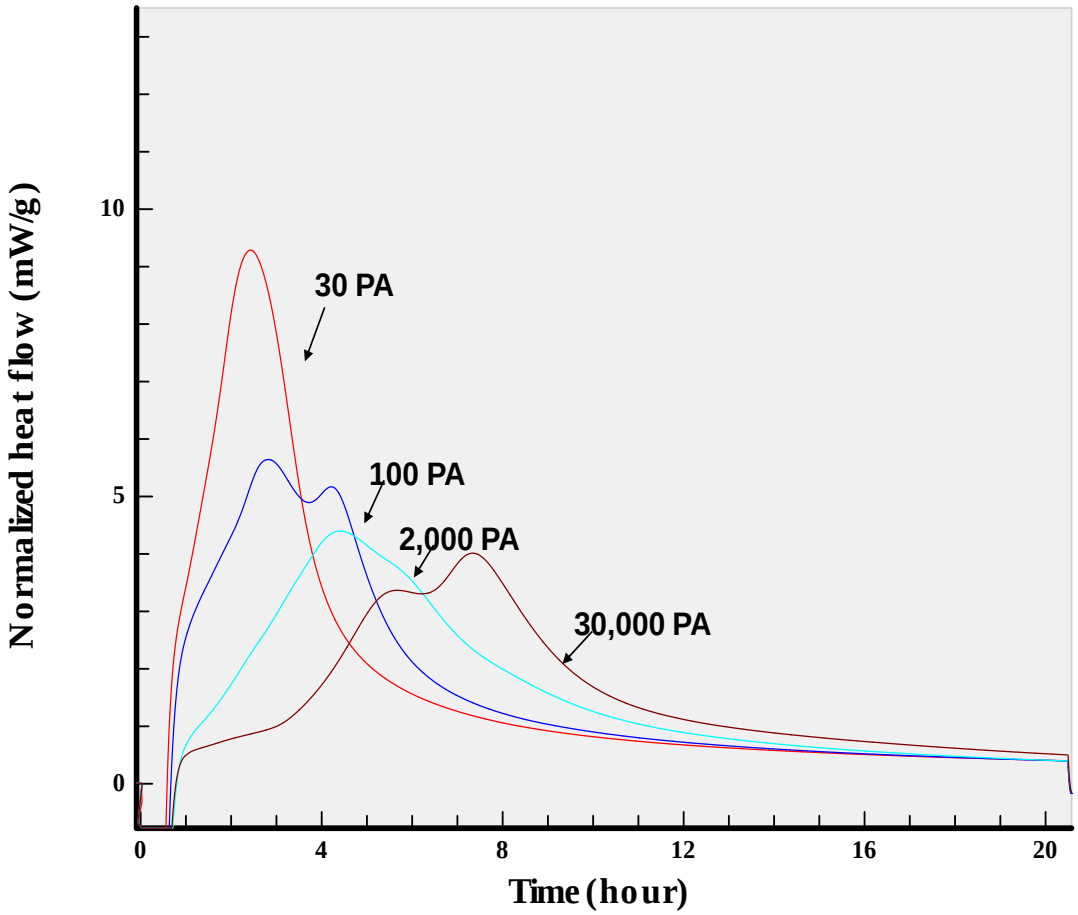

Fig. 2. Microcalorimetric curves of 30, 100, 2000, and 30000 PA CMC-modified sealer slurries at an isothermal temperature of 85°C.

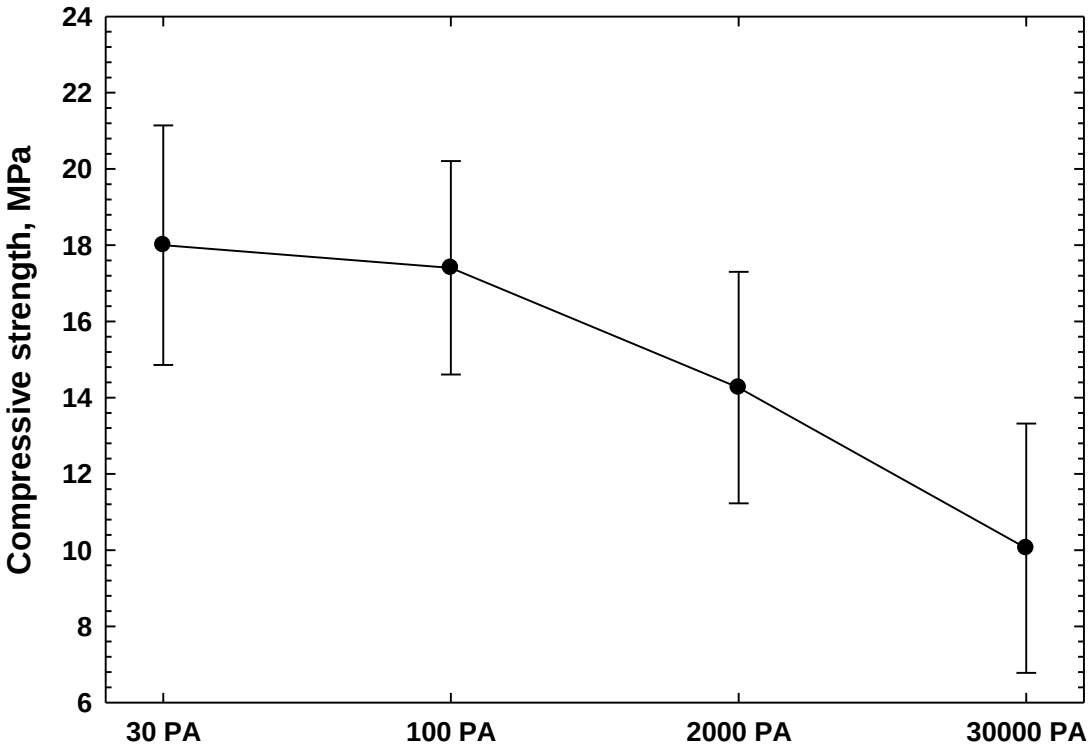

Fig. 3. Compressive strength of 85°C-autoclaved sealers containing 30, 100, 2000, and 30000 PA CMC.

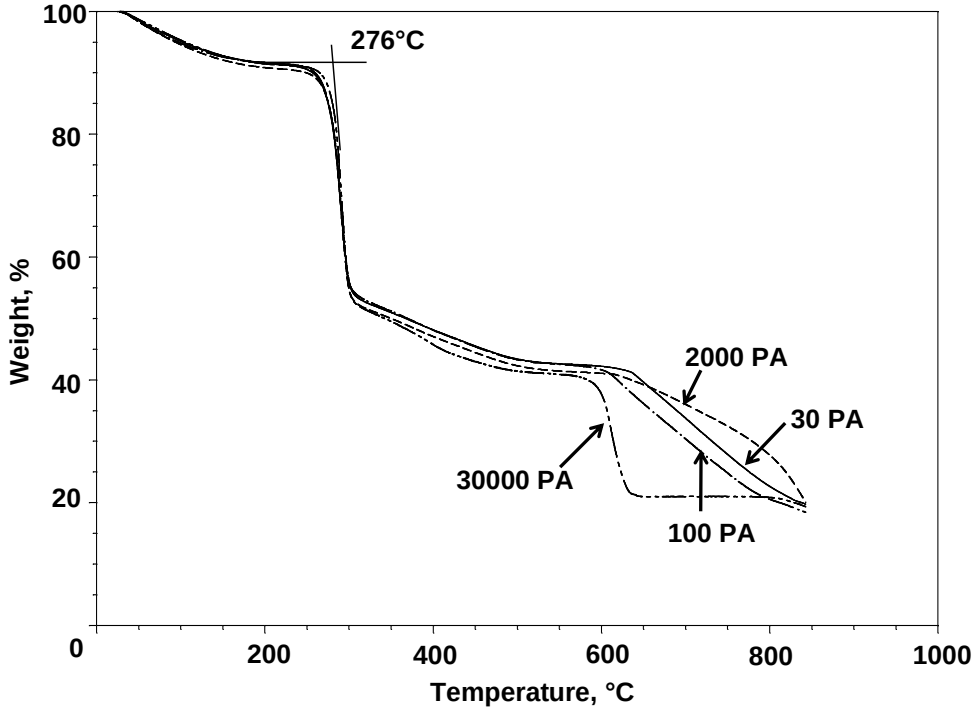

Fig. 4. TGA curves for "as-received" 30, 100, 2000, and 30000 PA CMCs.

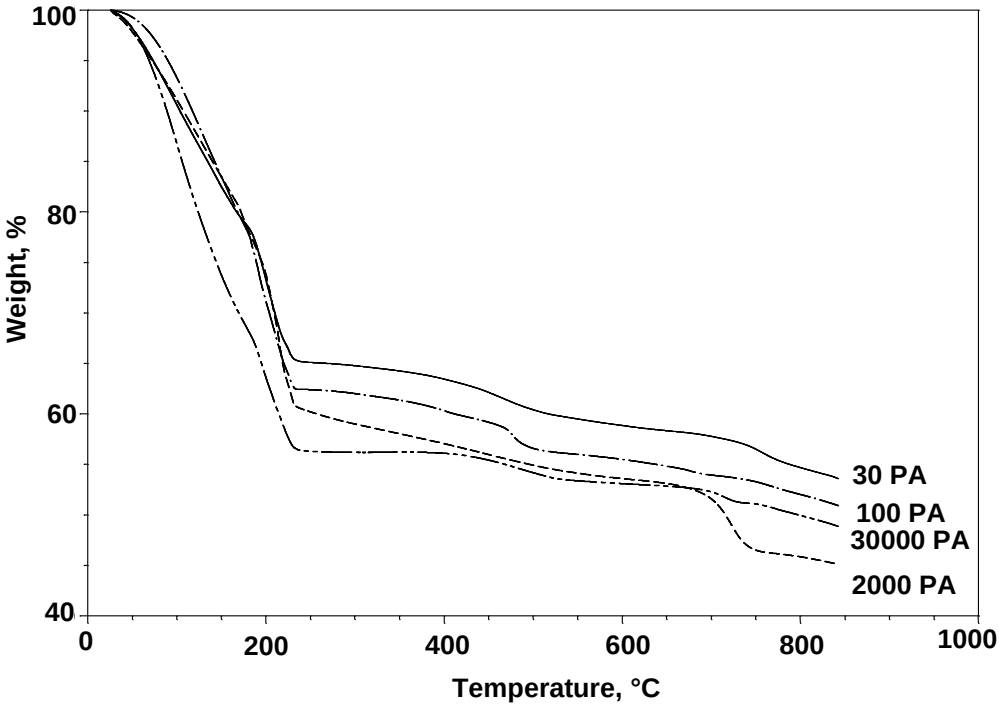

Fig. 5. TGA curves for pH 13.7 pore solution-treated CMCs at 200°C.

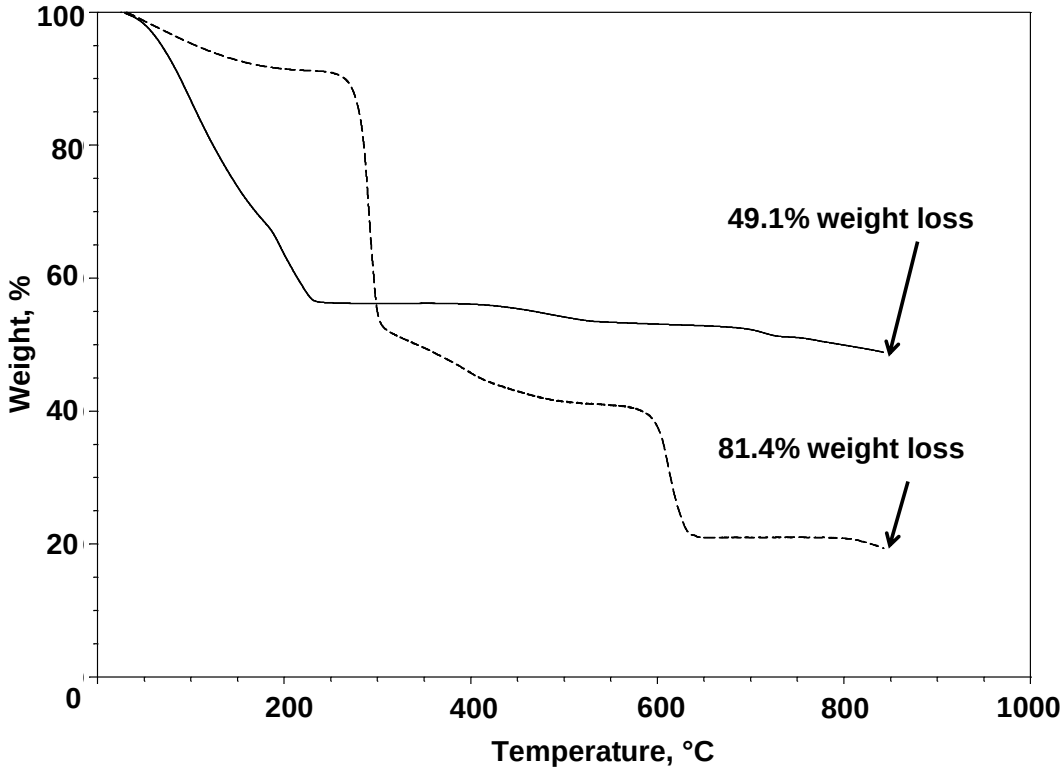

Fig. 6. Comparison of TGA curve for 30000 PA CMCs before (—) and after (----) the treatment with pH 13.7 pore solution at 200°C.

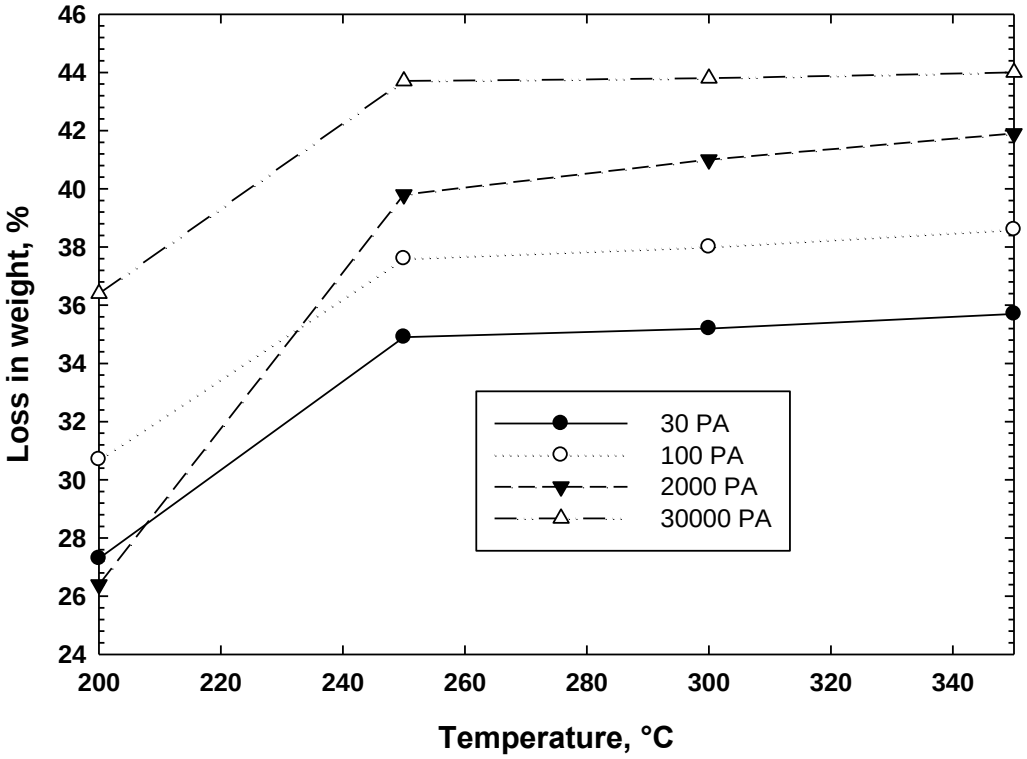

Fig. 7. Loss in weight of 200°C pore solution-treated CMCs at temperatures 200° to 350°C.

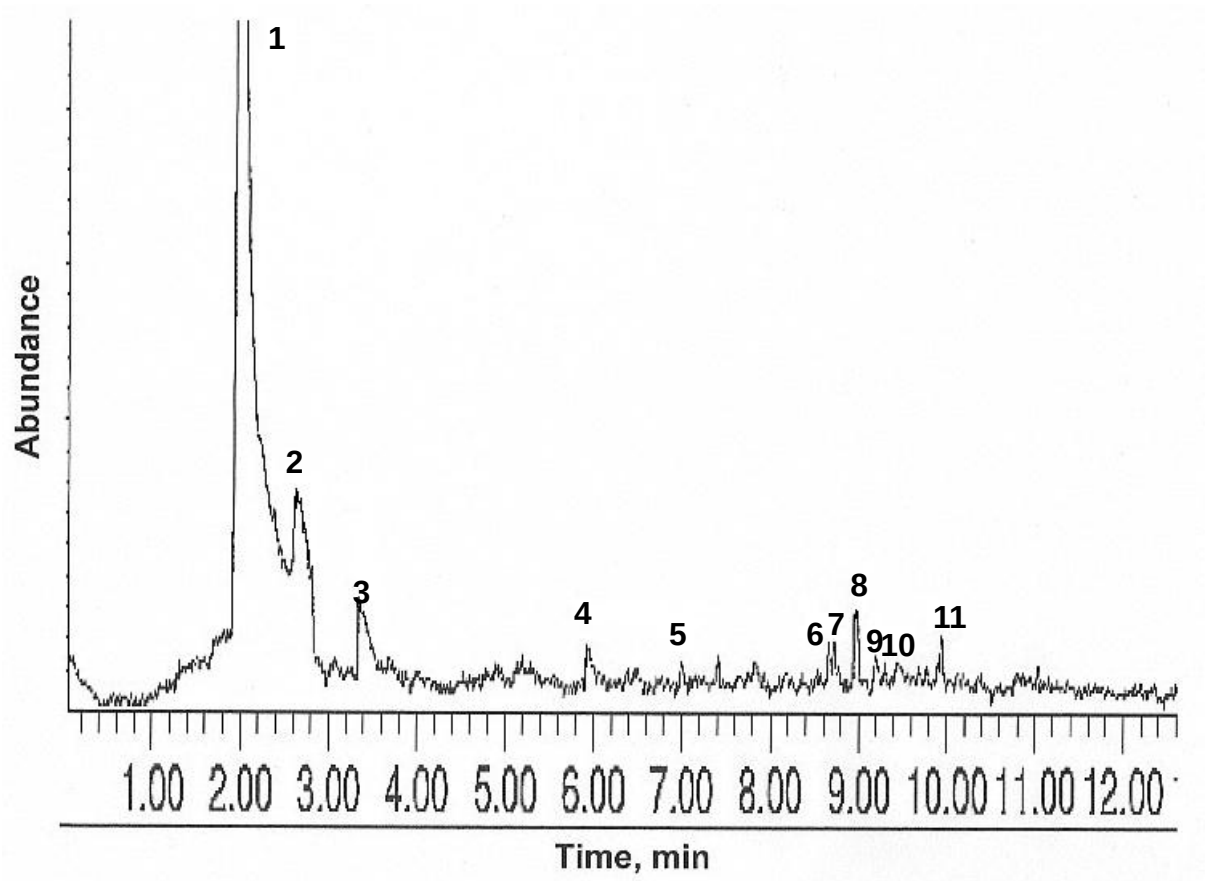

Fig. 8. Py-GC/MS abundance-retention time curve of 450°C -pyrolyzed 30000 PA CMC.

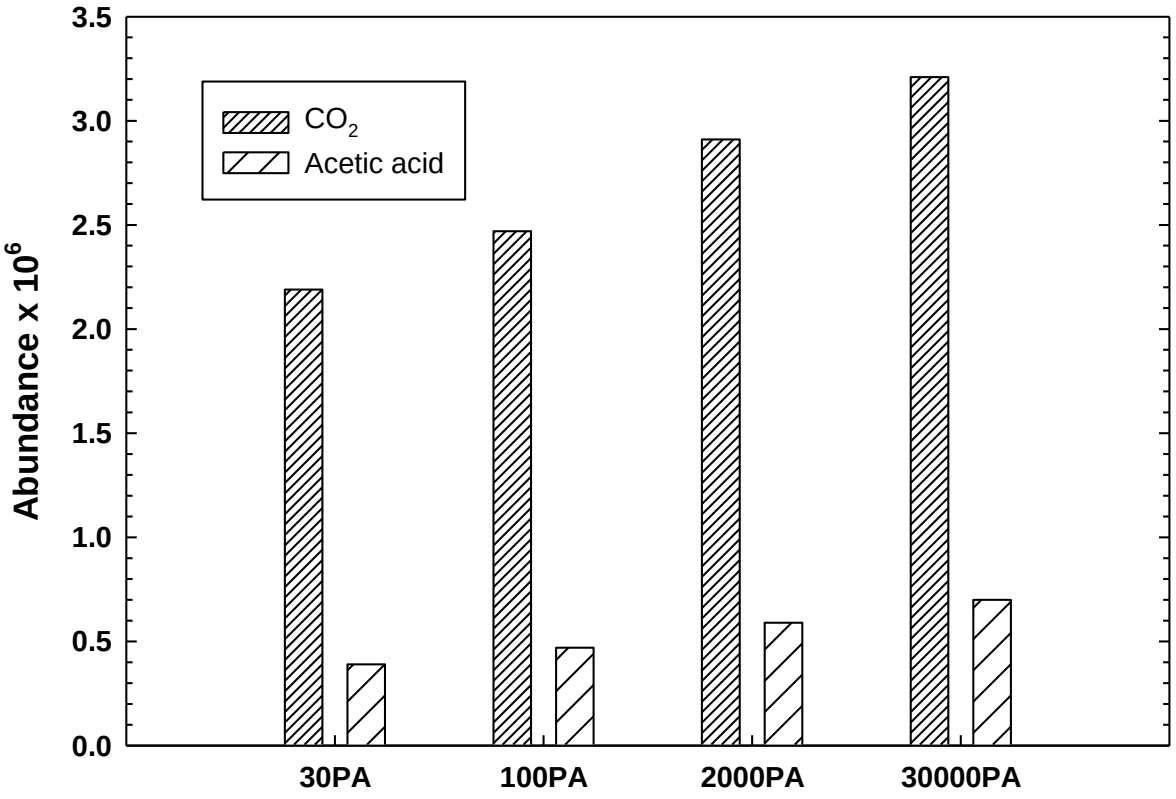

Fig. 9. Abundances of CO_2 and acetic acid emanated from 450°C-pyrolyzed 30, 100, 2000, and 30000 PA CMCs.

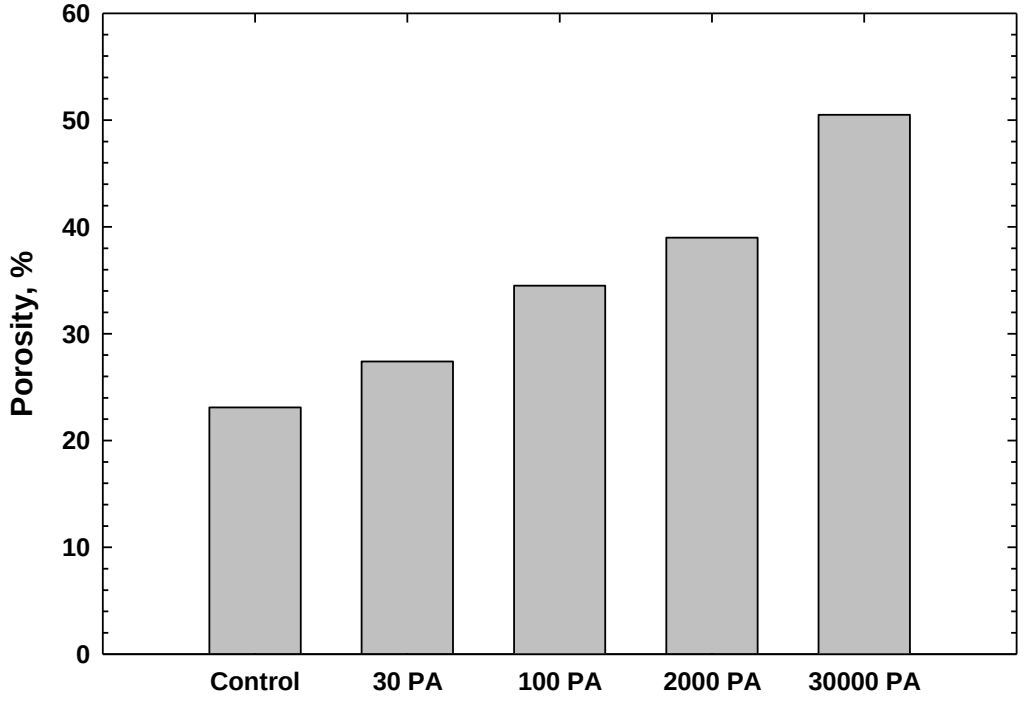

Fig. 10. Porosity of 85°C-autoclaved cements with and without various CMCs after heating at 200°C.

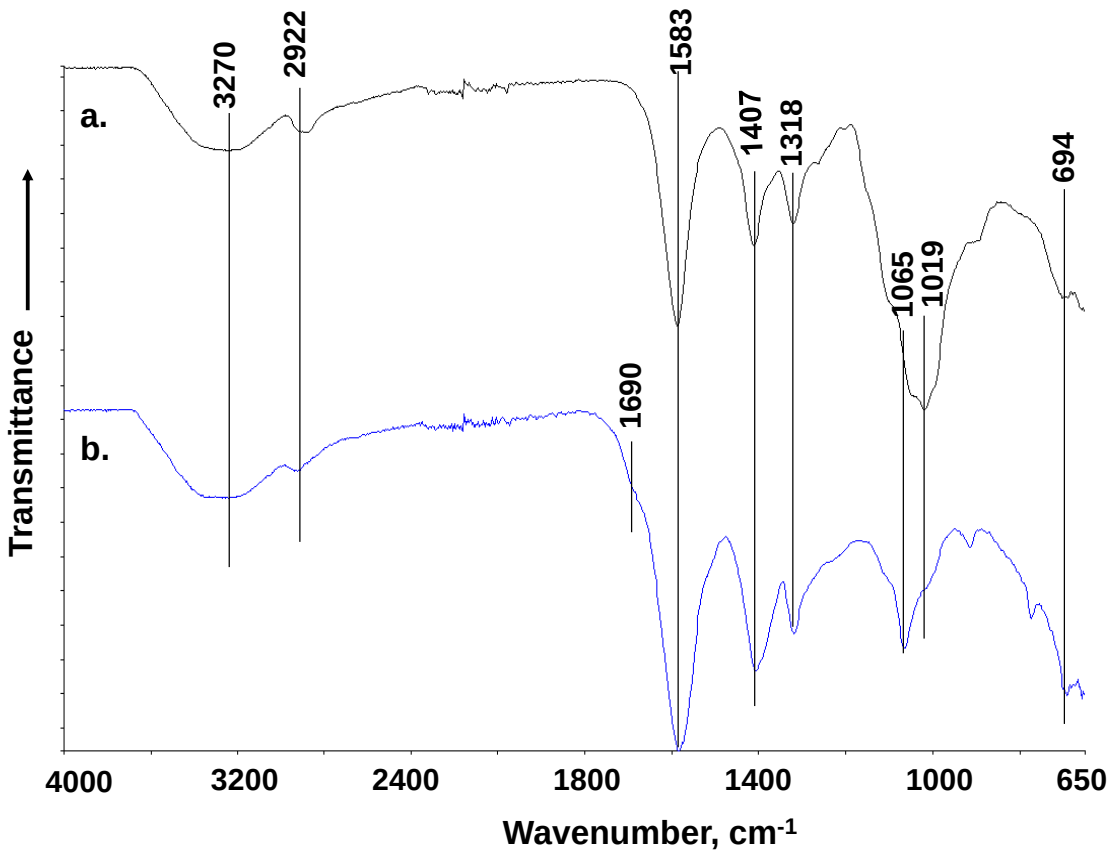

Fig. 11. FT-IR spectra of "as-received" (a), and 200°C-heated CMCs (b).

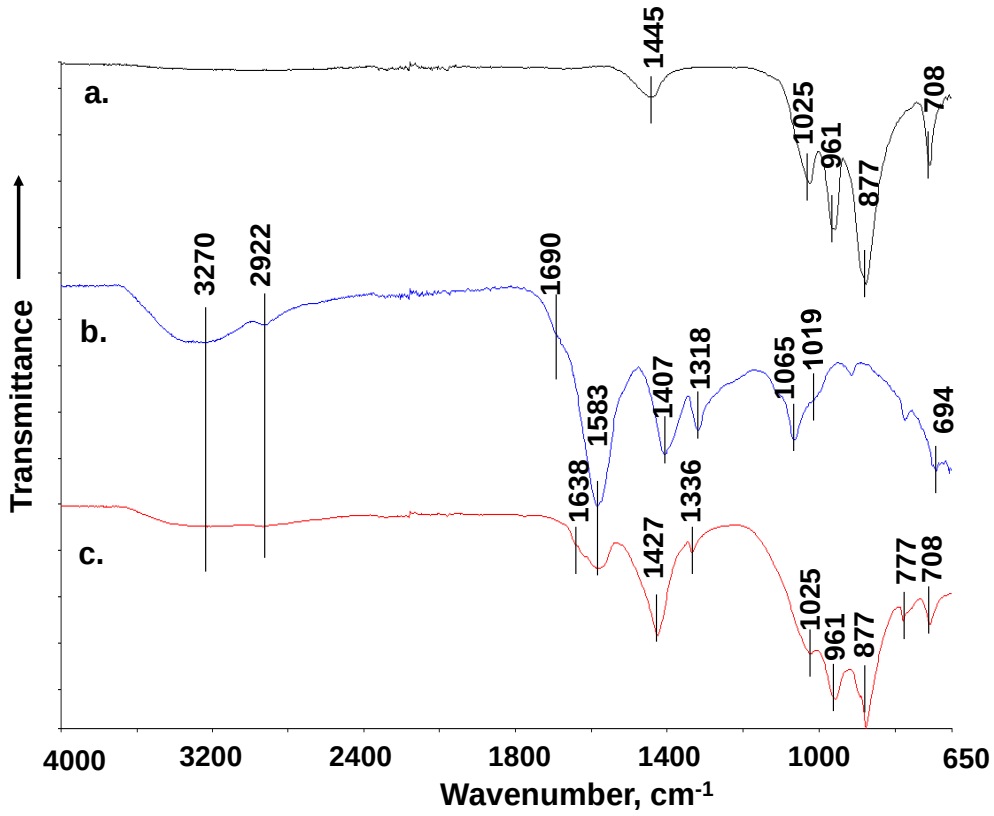

Fig. 12. Hypothetical scheme of CMC hydrothermal decomposition at 200^{o}C.

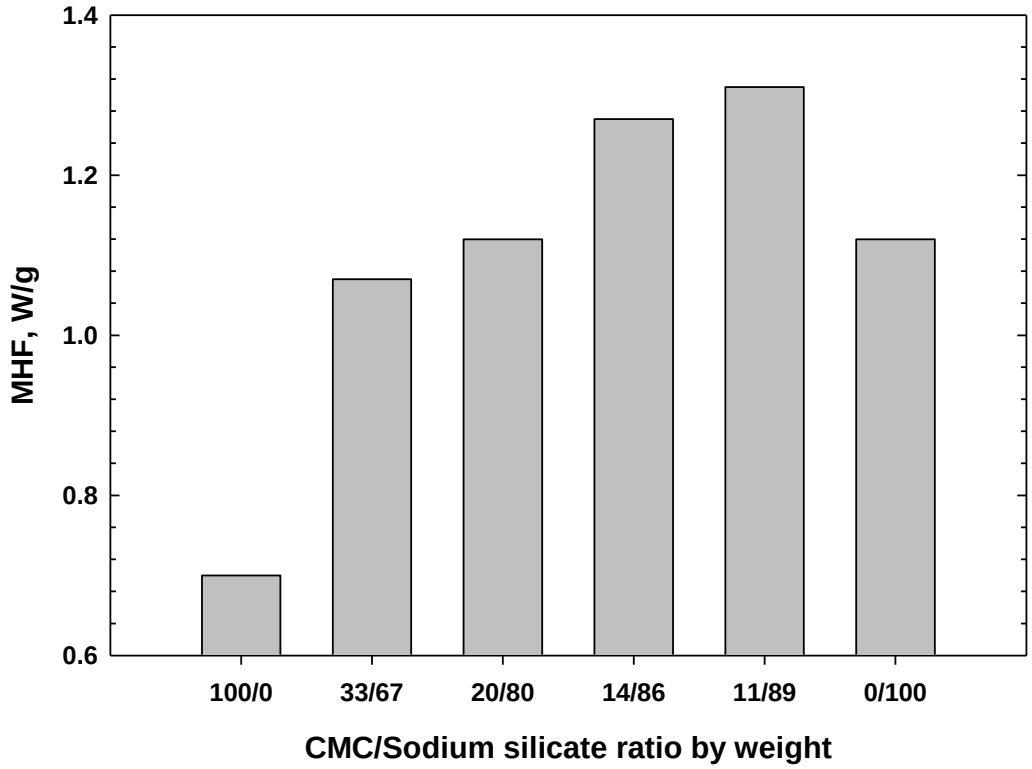

Fig. 13. Maximum heat flow (MHF, W/g) evolved from 200°C-heated 100/0, 33/67, 20/80, 14/86, 11/89, and 0/100 CMC/sodium silicate samples after mixing with water.

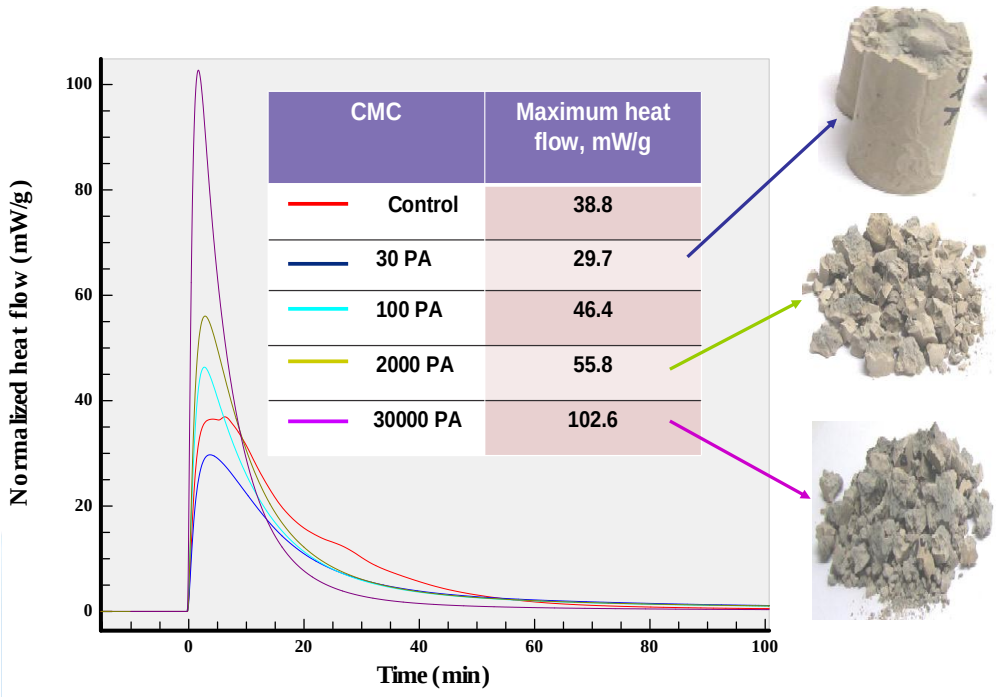

Fig. 14. Comparison of self-degradation performances for cements modified with different CMCs.